# STM of the (010) surface of orthorhombic phosphorus

Shueh-Lin Yau, Thomas P. Moffat, Allen J. Bard
*Department of Chemistry and Biochemistry, The University of Texas at Austin Austin, TX 78712, USA*

Zhengwei Zhang and Michael M. Lerner
*Department of Chemistry, Oregon State University, Corvallis, OR 97331, USA*

Received 30 April 1992; in final form 24 July 1992

Scanning tunneling microscopy (STM) was used to image the freshly cleaved (010) surface of orthorhombic black phosphorus (BP) in air. The surface became oxidized and adsorbed moisture from the air. The hydrophilic and reactive nature resulted in a rough and changing surface, as revealed by the STM. During STM imaging the BP surface was continuously removed by the W probe in a layer-by-layer fashion. Nevertheless, high quality STM atomic resolution images were obtained after the tip inscribed a depression by locally etching away several layers on the substrate. The puckered nature of the surface structure and the associated [100] oriented channels were clearly observed. Higher resolution imaging revealed the zig-zag arrangement of phosphorus atoms separated by about 0.22 nm.

Orthorhombic black phosphorus (bp) is the most stable allotropic form of the element under normal conditions [1,2]. The material is semiconducting with an optical gap of 0.3 eV. Its structure consists of puckered layers stacked in the [010] direction, as shown in fig. 1 [2,3]. Like many other two-dimensional solids, black phosphorus can be easily cleaved to expose the (010) surface. One reason we were interested in this material was its reported atomically flat surface, which could serve as a good substrate material in STM imaging experiments. Furthermore, BP provides a potential advantage over highly oriented pyrolytic graphite (HOPG) as a substrate by providing reactive sites to facilitate surface chemical bonding. These can enhance the adsorbate–substrate interaction so that the adsorbate will not be moved by the STM probe during the imaging process. The weak interaction between adsorbate and a substrate like HOPG has been a principal difficulty for STM imaging of isolated molecules. This report presents a preliminary study of the STM of BP. In the course

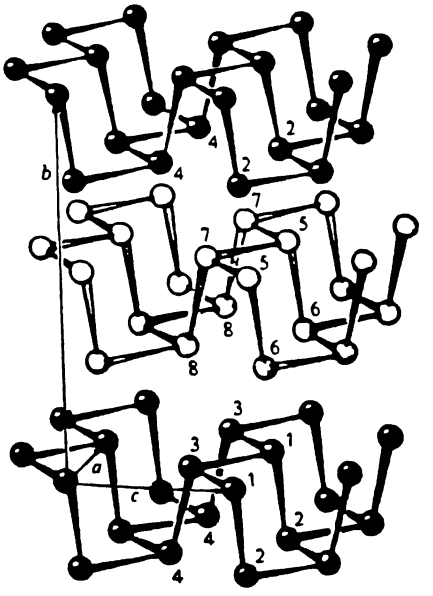


Fig. 1. Puckered layer structure for the orthorhombic black phosphorus. Bond distances, 1–2, 3–4, 5–6, 7–8: 0.2244 nm; 5–7, 1–3: 0.2224 nm; 3–8, 4–7: 0.3559 nm; 3–6, 2–7: 0.3769 nm. Bond angles, 1–3–1, 5–7–5: 96.34°; 7–5–6, 5–7–8, 4–3–1, 3–1–2: 102.09° (figure from ref. [2]).

*Correspondence to:* A.J. Bard, Department of Chemistry and Biochemistry, The University of Texas at Austin, Austin, TX 78712, USA.

of this study we observed layer-by-layer etching of the surface that was induced by the STM imaging process. We have utilized this etching process to fabricate a simple 1.0 nm deep, 20×20 nm rectangular pit on the (010) surface. We then obtained atomic resolution of the (010) surface of BP by imaging the depressed region.

Orthorhombic phosphorus can be fabricated by two different synthetic routes. High pressure methods pioneered by Bridgman [4] are commonly used, and precipitation from a liquid bismuth–phosphorus alloy has also been reported [3]. For the present investigation needle-shaped crystals, typically 7 mm× 0.5 mm×1 mm, were obtained by the precipitation scheme. Further details on this method and the product yield will be published elsewhere [5]. X-ray microprobe and Auger analysis demonstrated the elemental nature of the material, and the crystal structure (space group Cmca, $a=3.31$, $b=10.54$, $c=4.36$) confirmed by the X-ray rotating crystal method. In agreement with prior work, the needle axis was coincident with the [100] direction. For STM analysis the crystals were attached to platinum foil with silver paint. The [100] needle axis was oriented parallel to the $y$-scan direction of the microscope. The sample was routinely cleaved, immediately before imaging, with adhesive tape (Scotch). Imaging was performed in air with a Digital Instruments Nanoscope II STM (Santa Barbara, CA). Tunneling tips were made by mechanically cutting $Pt_{80}Ir_{20}$ wire or electrochemically etching tungsten wire in 1 M KOH.

In contrast to the inert van der Waals nature of

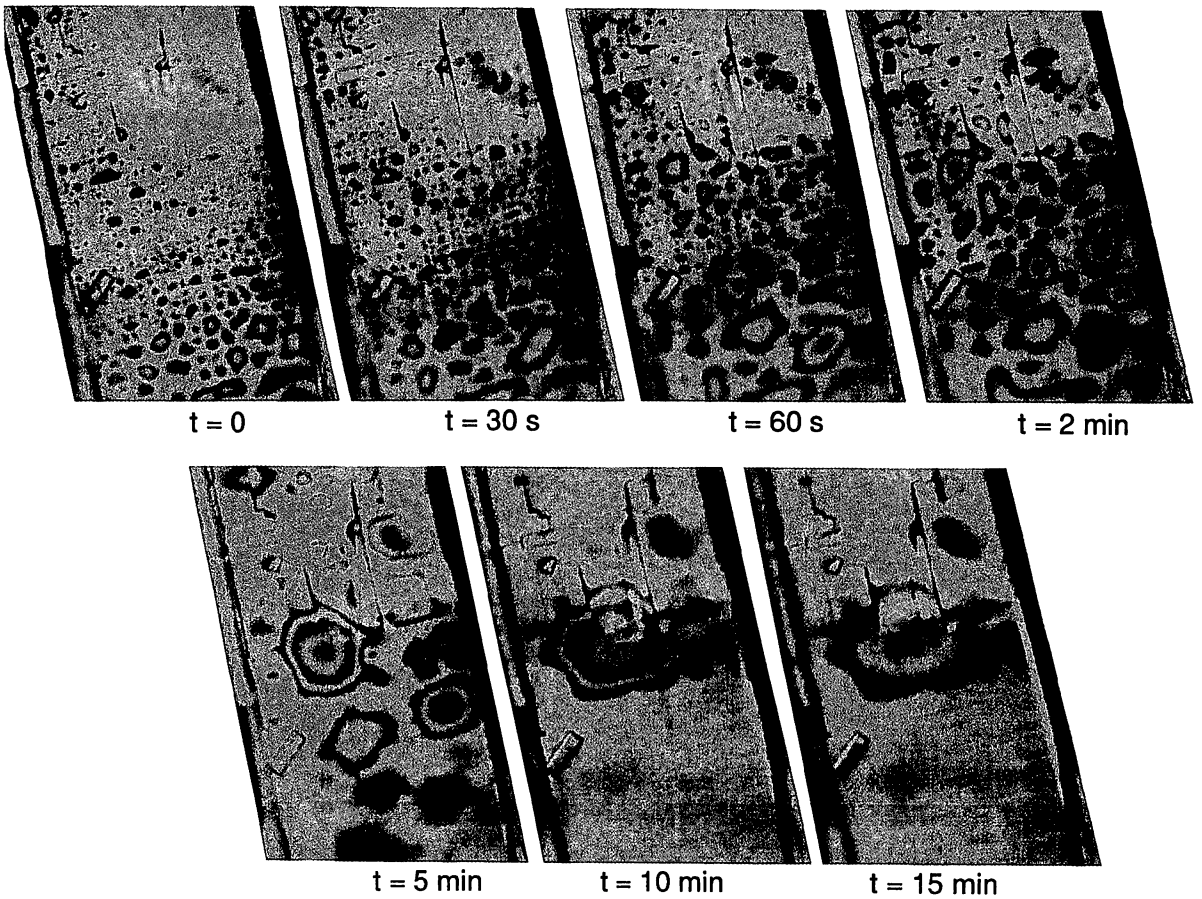


Fig. 2. Optical micrographs (magnification 500×) of freshly cleaved black phosphorus surface exposed to air.

many-layer-type materials, the BP surface is reactive in air. When the surface was examined by optical microscopy, inhomogeneities that changed with time were seen. Some regions exhibited a mirror-like surface while others had a duller appearance and showed changing interference colors (fig. 2). These surface features resemble the breath figures [6] arising from the condensation of moisture on a solid substrate. When BP was imaged in air with the STM, with electrochemically etched probes (W or Pt/Ir alloy) the formation of bubbles at the tip was often seen as the tip approached the tunneling distance to the BP substrate. This was observed only when the W tip was biased +0.60 V or more with respect to the BP sample. However, with Pt/Ir tips, gas evolution was observed with either tip polarity when the bias was higher than +0.60 V. These results are consistent with the formation of a thin layer of water on the BP surface. This would occur when the BP is oxidized in air to produce a strongly hydrophilic $P_4O_{10}$ oxide layer [7],

$$P_4 + 5O_2 \rightarrow P_4O_{10}\,, \qquad (1)$$

which readily reacts with moisture in the air,

$$P_4O_{10} + 6H_2O \rightarrow 4H_3PO_4\,. \qquad (2)$$

This reaction mechanism is supported by the results from scanning Auger spectroscopy, which indicates the presence of oxygen and an oxidized form of phosphorus on the BP surface after exposure to air. This passivating oxide layer is probably responsible for the stability of BP in the ambient environment.

Electrochemical reactions at the tip and BP probably produce the bubbles seen in the STM experiments. With a W tip the following reactions are thermodynamically possible:

At anode (W tip):

$$W + H_2O \rightarrow WO_3 + 6H^+ + 6e^-\,,$$

$$E^0 = +0.10\ \text{V}\ [8]\,, \qquad (3)$$

$$H_2 \rightarrow 2H^+ + 3e^-\,, \qquad (4)$$

$$PH_3 + 4H_2O \rightarrow H_3PO_4 + 8H^+ + 8e^-\,,$$

$$E^0 = +0.281\ \text{V}\ [8]\,, \qquad (5)$$

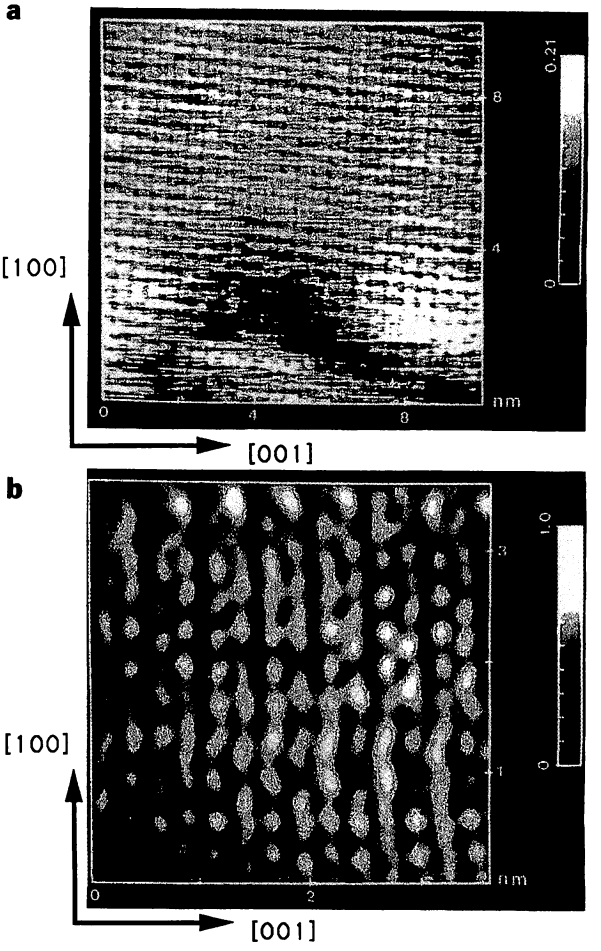


Fig. 3 (a) An unfiltered STM image shows the channels running along the (100) direction of the (010) plane of black phosphorus. The image was obtained at a bias of 20 mV and tunneling current of 5 nA. Two neighboring troughs are separated by 0.43 nm which matches with the *c*-axis dimension. (b) An enlarged and filtered STM atomic resolution image of the layered BP. The image was also obtained at 20 mV and 5 nA, and a two-dimensional Fourier transform filtering method was used to removed spatial frequencies below 0.20 nm.

At cathode (BP):

$$P + 3H^+ + 3e^- \rightarrow PH_3\,,$$

$$E^0 = +0.10\ \text{V}\,, \qquad (6)$$

$$2H^+ + 2e^- \rightarrow H_2\,. \qquad (7)$$

Gas evolution lasted for more than 5 min in the STM, so that reactions (1) and (2) must be sufficiently rapid to form a water layer and $H^+$ to allow reac-

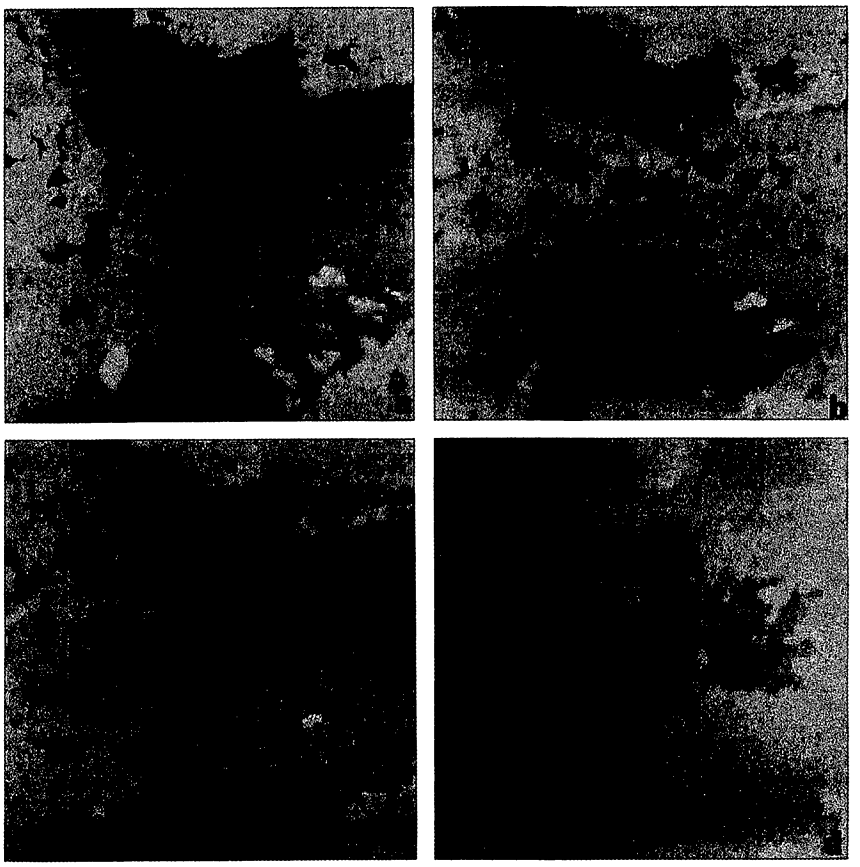

Fig. 4. A sequence of images revealing the progressive layer-by-layer etching of black phosphorus after (a) 0, (b) 50, (c) 100 and (d) 240 s. These images were obtained with a 300 mV bias voltage and 1.0 nA tunneling current.

tions (6) and (7) to occur. These lead to the formation of $PH_3$ and $H_2$, both of which are colorless gases. The oxidation half-reactions at the W tip electrode could include oxidation of the W tip, or oxidation of $H_2$ or $PH_3$ coming from the BP substrate. The failure to observe bubbling at a W probe cathode can be explained by the difficulty of reducing $H^+$ (high hydrogen overpotential) on the W. However, at a Pt/Ir tip, water can be both reduced and oxidized. For the BP, the reduction processes would still be described by eqs. (5) and (6), while a possible oxidation process is

$$P+4H_2O \rightarrow H_3PO_4+5H^+ +5e^- ,$$
$$E^0 = +0.40\ \text{V} . \qquad (8)$$

Better evidence for the proposed reactions at the BP surface await futher electrochemical studies. We might note that electrolysis of water adsorbed from the atmosphere on a thin $P_4O_{10}$ layer has been used for water analysis [9].

Even with the BP surface instability, atomic resolution images of the (010) surface could be obtained (fig. 3). These images were taken in the constant current mode with a relatively high tunneling current (5 nA) and a small bias voltage (+20 mV, tip versus sample). This low bias voltage, compared to the band gap of BP (0.30 eV), suggests that the STM was imaging in a point-contact mode [10] where the tip was in contact with the surface. This presumably distorts the surface lattice and shifts states into the band gap which then participate in the

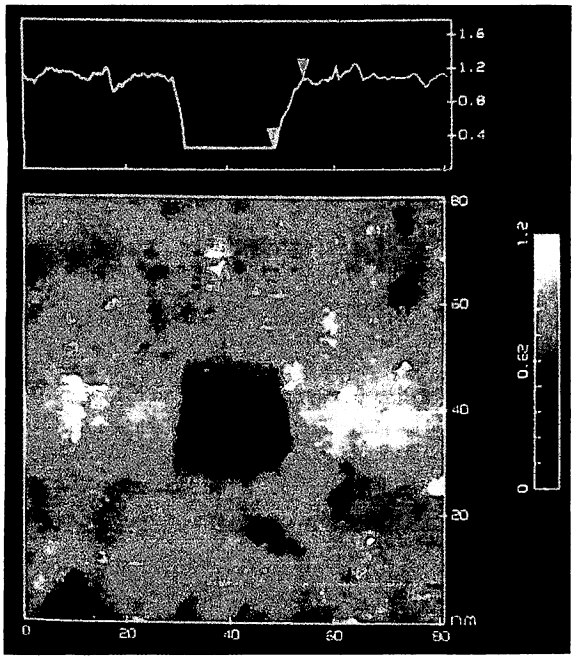


Fig. 5. A square (20 nm×20 nm) pit produced by STM scanning at 200 mV and 1 nA for two min. The depth of this inscribed depression (1.0 nm) corresponds to the unit length of the *b* vector. A line scan across the etched square pit is shown at the top of the image.

tunneling process. Similar effects were previously documented to explain the atomic resolution of layer-type semiconductors, such as $MoS_2$ [11] and others [12]. In the present case the distortion of the atomic image and the stray noise in the *x*-scan direction are consistent with this proposed mechanism (fig. 3). However, the puckered nature of the (010) surface is clearly demonstrated by the channels running vertically through the image shown in fig. 3a. These troughs are parallel with the [100] direction and are separated by about 0.43 nm, which corresponds to the (001) unit cell dimension. The high resolution image shown in fig. 3b reveals the [100] zig-zag arrangement of phosphorus atoms on the topmost portion of the puckered (010) surface. The phosphorus atoms are separated by about 0.22 nm with a bond angle of 96°. Resolving the electron density associated with individual phosphorus atoms is challenging in view of the small separation. Atomic resolution of the trough segment of the puckered layer was not obtained. Presumably the narrow trough width (0.30 nm) prevents the tunneling tip from probing the lower (0.24 nm) portion of this layer. This also accounts for the anomalously shallow depths (0.070 nm) measured for the troughs.

The freshly cleaved surface has wide terraces, extending several hundred nanometers, with a high density of vacancy clusters apparent in these layers. (fig. 4). These defects and the steps separating each terrace are $\approx 1.1$ nm deep; this corresponds to the (010) unit cell dimension or two puckered layers. Progressive scanning revealed significant lateral growth of these defects. An area spanning $\approx 200$ nm$^2$ could be removed by four min of scanning, as shown in fig. 4. The material etched away is either transferred to the tip or volatilized. The etch rate increased with decreasing tip–substrate separation and decreasing bias. Indeed, it was difficult to find tunneling conditions where this process did not occur. Therefore, high-quality STM images of the (010) surface like those in fig. 3 were difficult to obtain on a routine basis; more frequently strong tip–surface interactions caused the layer-by-layer removal of substrate material. This etching process could be used to form a hole of predetermined dimensions, e.g., a 1.0 nm deep pit on the (010) surface. The inscribed pit shown in fig. 5 was produced by scanning a 20 nm×20 nm area for 2 min. Similar structures have been fabricated on other two-dimensional solids [6]. Similar etching phenomena have also been observed for other two-dimensional solids, e.g., $TiSe_2$, $SnSe_2$, and $NbSe_2$ [13]. Several mechanisms for the etching process have been proposed, e.g., abrasion of the substrate via direct tip–sample contact [14] and field assisted evaporation [15]. In the experiments described here there was considerable variation in the etching rate with different tips, and it was thus difficult to elucidate the effect of different tunneling conditions on the etching. The high resolution images, e.g., fig. 3, probably were obtained, when the STM probe was scanning within a narrow pit on the BP substrate, where the tip might block incoming reactants. Finally, this study suggests that the surface of BP is probably too reactive in air to serve as a useful substrate for imaging of isolated molecules by STM, although its use in an inert atmosphere might be possible.

## Acknowledgement

The support of this research by grants from the Texas Advanced Research Program and the Office of Naval Research is gratefully acknowledged. We thank Dr. Fu-Ren F. Fan for helpful discussions.

## References

[1] N.B. Goodman, L. Ley and D.W. Bullett, Phys. Rev. B. 27 (1983) 7440.
[2] T. Kikegawa and H. Iwasaki, Acta Cryst. B 39 (1983) 158.
[3] A. Brown and S. Rundqvist, Acta Cryst. 19 (1965) 684.
[4] P.W. Bridgman, J. Am. Chem. Soc. 36 (1914) 1344.
[5] Z. Zhang and M. M. Lerner, to be submitted for publication.
[6] B.J. Briscoe and K.P. Galvin, Colloids Surfaces 56 (1991) 263.
[7] J.D. Lee, Concise inorganic chemistry, 4th Ed. (Chapman & Hall, New York, 1991) p. 475.
[8] A. J. Bard, ed., Encyclopedia of electrochemistry of the elements, Vol. 3 (Marcel Dekker, New York, 1975) p. 3.
[9] F.A. Keidel, Anal. Chem. 31 (1959) 2043;
L.G. Cole, M.C. Zuha, R.W. Mosley and D.T. Sawyer, Anal. Chem. 31 (1959) 2048.
[10] J.H. Coombs and J.B. Pethica, IBM J. Res. Develop. 30 (1986) 455;
H.J. Mamin, E. Ganz, D.W. Abraham, R.E. Thomson and J. Clarke, Phys. Rev. B. 34 (1986) 9015;
S. Ciraci and E. Tekman, Phys. Rev. B 40 (1989) 11969.
[11] W.M. Heckl, F. Ohnesorge and G. Binnig, J. Vacuum Sci. Technol. B 9 (1991) 1072.
[12] M.B. Salmeron, D.F. Ogletree, C. Ocal, H.-C. Wang, G. Neubauer, W. Kolbe and G. Meyers, J. Vacuum Sci. Technol. A 9 (1991) 1347.
[13] B. Parkinson, J. Am. Chem. Soc. 112 (1990) 7498.
[14] E. Garfunkel, G. Rudd, D. Navak, S. Wang, G. Ebert, M. Greenblatt, T. Gustafsson and S.H. Garofalini, Science 246 (1989) 99.
[15] T. Sakurai, A. Sakai, and H. W. Pickering, Atomic-probe field ion microscopy and its applications (Academic Press, New York, 1989) p. 9.